Microglial responsiveness to hyperexcitable human iPSC-neurons carrying epilepsy-associated sodium channel Nav1.2 genetic variant

Zhefu Que[1], **Maria Olivero-Acosta**[1], Jingliang Zhang[1], Kyle W Wettschurack[1],Xiaoling Chen[1], Yuanrui Zhao[1], Ian Chen[1], Tiange Xiao[1], Jiaxiang Wu[1], Brody Deming[1], William Skarnes[2], Yang Yang[1*];

Department of Medicinal Chemistry and Molecular Pharmacology, Purdue University[1]. The Jackson Lab[2]

Advancing pharmacogenomics to cure diseases of the nervous system and cancer

Introduction

Nav1.2, a voltage-gated sodium channel encoded by *SCN2A*, is responsible for action potential firing and propagation in the central nervous system. Due to the wide adoption of whole-genome sequencing over the past few years, a strong association has been established between genetic variants of *SCN2A* and a wide range of neurological diseases including epilepsy, autism spectrum disorder (ASD) and intellectual disability among others *(Begemann et al., 2019).* To understand how major recurring variants of *SCN2A* perturb neurons and alter neuronal excitability, we used CRIPSR/Cas9 to create an *SCN2A* disease-associated variant: p.L1342P in a human reference iPSC line (KOLF2-C1), a line with defined genetic lineage, reducing unwanted influence by patient-specific backgrounds. This recurring variant detected in 5 patients *(Matalon, 2014; Hackenberg, 2014; Dimassi, 2016; Wolff, 2017)*, has been associated with early-onset epileptic encephalopathy, which manifests as very severe and intractable seizures. The data we present support the feasibility of using iPSC disease models to elucidate mechanisms of disease specifically caused by *SCN2A* variants and provide information for personalized treatment (for detailed information, please refer our paper recently published on *Journal of Neuroscience, 2021*).

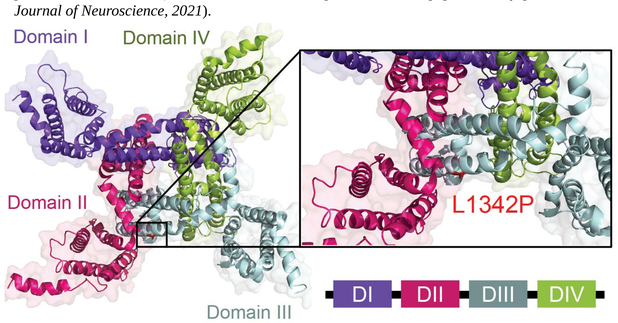

Figure 1. Schematic 3D-Structure of Nav1.2 Sodium Channel. Mutated residue L1342P is indicated by zoomed-in box. Modified from PDB ID: 6J8E *(Pan et al., 2019)*

Methods

Schematic protocol and the timeline for cortical neuron and microglia differentiation

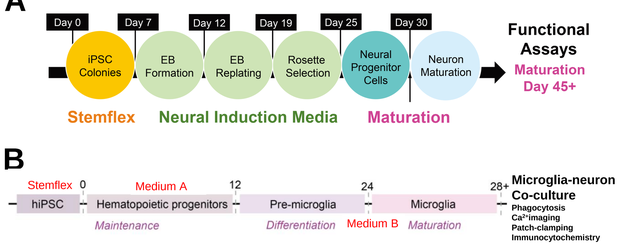

Figure 2. Flowchart depicting the stepwise differentiation protocol for cortical neurons and microglia. (**A**) Reference line iPSCs were differentiated for 45 days into cortical neurons. (**B**) The hematopoietic progenitors were first generated, and then further give rise to mature microglia for microglia differentiation. The microglia would then be used in downstream experiments including phagocytosis and co-culture with neurons..

iPSC-derived neurons/microglia express specific markers

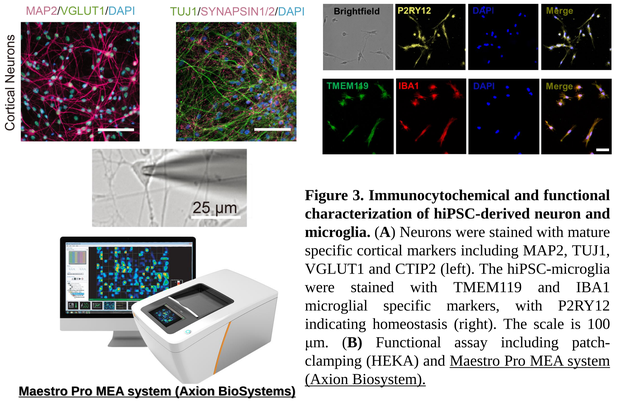

Figure 3. Immunocytochemical and functional characterization of hiPSC-derived neuron and microglia. (**A**) Neurons were stained with mature specific cortical markers including MAP2, TUJ1, VGLUT1 and CTIP2 (left). The hiPSC-microglia were stained with TMEM119 and IBA1 microglial specific markers, with P2RY12 indicating homeostasis (right). The scale is 100 µm. (**B**) Functional assay including patch-clamping (HEKA) and Maestro Pro MEA system (Axion Biosystem).

Results

Nav1.2-L1342P variant displays complex biophysical properties

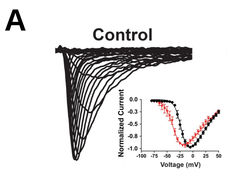

Figure 4. Representative traces of whole-cell sodium current from HEK cells expressing control Nav1.2 or Nav1.2-L1342P channel. (A) Sodium current traces for control. **(B)** Sodium current traces for Nav1.2-L1342P. The inset depicts the normalized current-voltage (I-V) curve.

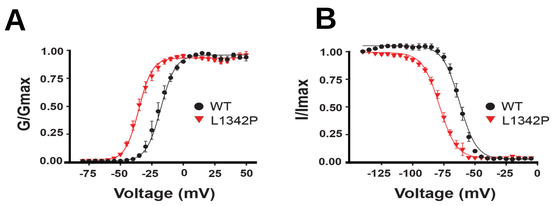

Figure 5. Voltage-dependent activation (A) and steady-state fast inactivation (B) of WT and Nav1.2-L1342P mutant channels. (A) L1342P variant causes a left-shift around 17 mV, indicating a gain-of-function phenotype. **(B)** In fast-inactivation, L1342P variant caused a left-shift, indicating a loss-of-function phenotype.

The Nav1.2-L1342P variant increases the intrinsic excitability of hiPSC-derived neurons

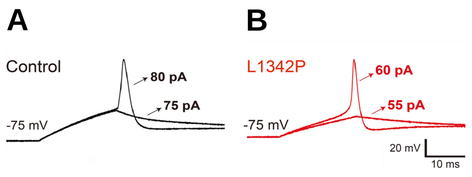

Figure 6. Representative action potential firings from iPSC-derived neurons. (**A**) Representative brightfield image of a hiPSC-derived pyramidal-shaped neuron selected for patch-clamp experiments. (**B**) and (**C**) Representative single action potential triggered by a stepwise increment of current stimulus with a 20 ms duration.

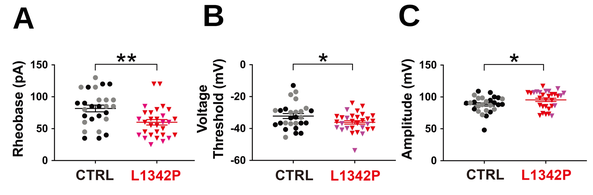

Figure 7. The hiPSC-derived neurons with Nav1.2-L1342P variant display increased excitability. (**A**) The L1342P variant reduced the minimal current needed for evoking an intact AP in neurons. (**B**) The voltage threshold of AP was hyperpolarized in L1342P neurons. (**C**) APs from neurons carrying the L1342P variant had an elevated peak amplitude. *Student's t-test.*

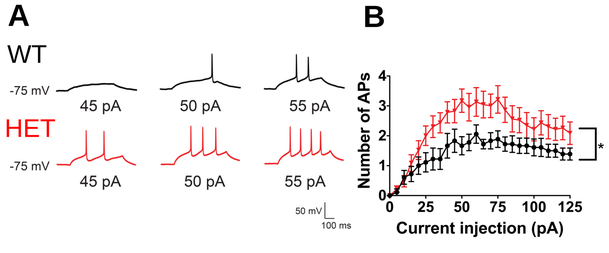

Figure 9. Repetitive firing properties recorded in hiPSC-neurons. (A) Sustained action potential firings. **(B)** AP number per epoch in response to graded current injection. Nav1.2-L1342P neurons consistently fired more APs than control neurons. Repeated-measures two-way ANOVA analysis.

Heightened neural network excitability, with reduced sensitivity in phenytoin treatment using neurons carrying the Nav1.2-L1342P variant

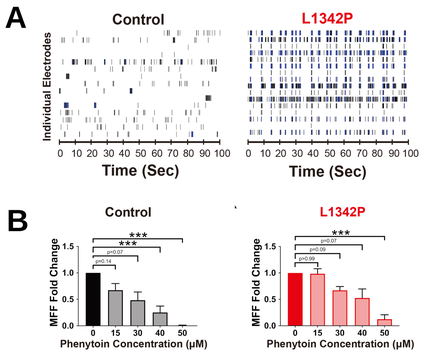

L1342P culture displays enhanced network excitability

L1342P culture shows features of drug-resistance in suppressing the firing frequency

Figure 10. Elevated network excitability revealed by micro-electrode array (MEA) recordings of L1342P culture (A) Representative raster plots of spikes generated for isogenic control and Nav1.2-L1342P cultures. **(B)** Inhibitory effects of different doses of phenytoin for isogenic control and L1342P cultures. Kruskal-Wallis test was performed with Dunn's multiple comparisons post hoc analysis.

Characterization of hiPSC-microglia and co-culture with hiPSC-neurons

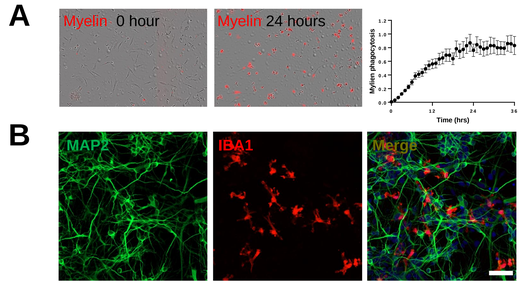

Figure 11: The hiPSC-derived microglia were able to perform a normal phagocytotic function and displayed ramified morphology in the co-culture system. (**A**) The microglia exhibited normal ability to internalize the myelin under the exposure of pHrodo-labeled myelin particles. (**B**) Representative images indicate human iPSC-derived microglia displayed a ramified morphology and have close contact with neurons.

Enhanced microglial calcium signal with a preference in process territory when co-cultured with endogenously hyperexcitable Nav1.2-L1342P neurons

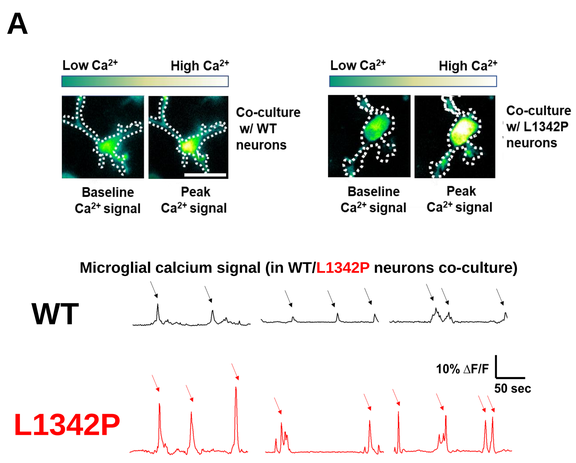

Results

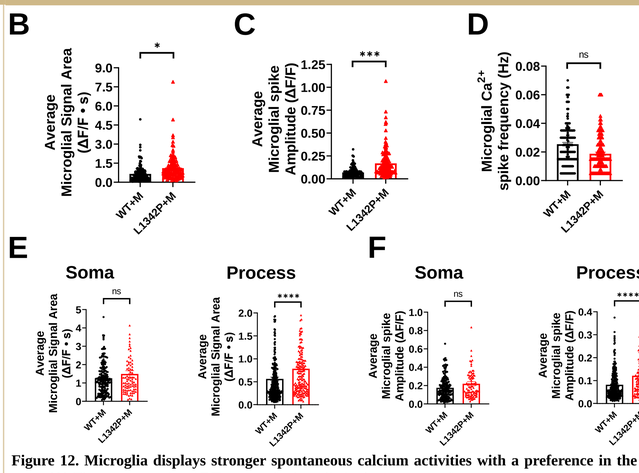

Figure 12. Microglia displays stronger spontaneous calcium activities with a preference in the process area. (A) The representative ΔF/F traces of microglia in the presence of neurons were generated from isogenic control and Nav1.2-L1342P hiPSCs. The inset represents the area of ROI from individual microglia for quantification. **(B-D)** The calcium signal area, average amplitude and spike frequency were recorded from microglia. **(E-F)** Comparison of calcium signal area and average amplitude between soma and process area.

Microglia exhibited extended process and higher branching complexity co-cultured with L1342P neurons

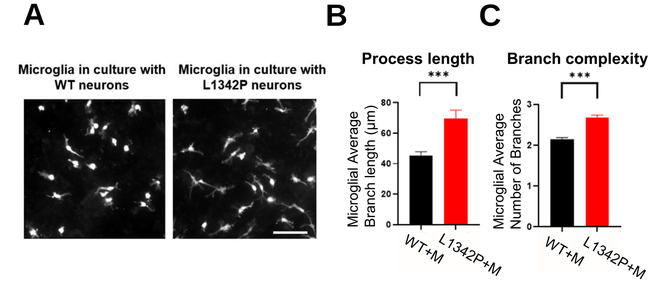

Figure 13. Microglia have a longer process with more ramified morphology in co-culture with L1342P neurons. (A) The representative microglia morphology when in culture with either WT or L1342P neurons **(B)** Average branch length of microglia in co-culture **(C)** Average branch complexity of microglia in co-culture. WT+M: wild-type neuron with microglia. Scale bar = 50 µm.

PSD95 engulfment in the microglia-containing cortical organoid

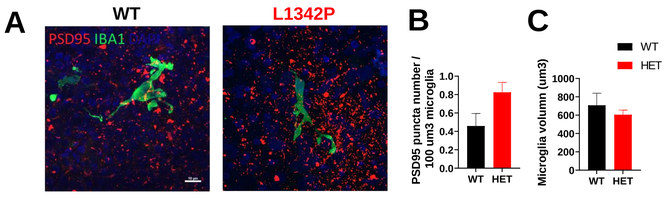

Figure 14. PSD95 engulfment in microglia. (A) Representative images showing PSD95 and IBA1 in the microglia-containing organoid. **(B)** Quantification of PSD95+ puncta (red) localized in the IBA1+ microglia (green).(**C**) Quantification of microglia volume in the cortical organoids.

Conclusions

- ❑ Neurons with Nav1.2-L1342P variant displays increased intrinsic and network excitability, with elevated current density, indicating a gain-of function phenotype.
- ❑ hiPSC-derived microglia cocultured with Nav1.2-L1342P neuron culture shows increased calcium activities and elongated process.

Acknowledgements

Part of this work was recently published with the *Journal of Neuroscience* (https://doi.org/10.1523/JNEUROSCI.0564-21.2021). Funding for this work is generously supported by the FamilieSCN2A foundation for the Action Potential Award; Yang Lab startup funding from Purdue University; Ralph W. and Grace M. Showalter Research Trust Award; NIH-NINDS R01NS117585; R01NS123154 and Purdue Discovery Park Big Idea Challenge.